Sensors and Actuators B 146 (2010) 183–189

Contents lists available at ScienceDirect

Sensors and Actuators B: Chemical

journal homepage: www.elsevier.com/locate/snb

C_2H_5OH sensing characteristics of various Co_3O_4 nanostructures prepared by solvothermal reaction

Kwon-Il Choi [a], Hae-Ryong Kim [a], Kang-Min Kim [a], Dawei Liu [b], Guozhong Cao [b], Jong-Heun Lee [a,*]

[a] Department of Materials Science and Engineering, Korea University, Anam-Dong, Sungbuk-Gu, Seoul 136-713, Republic of Korea
[b] Department of Materials Science and Engineering, University of Washington, Seattle, WA 98195, USA

ARTICLE INFO

Article history:
Received 20 October 2009
Received in revised form 4 February 2010
Accepted 15 February 2010
Available online 20 February 2010

Keywords:
Co_3O_4
Gas sensors
Nanostructures
C_2H_5OH sensor
Response/recovery time

ABSTRACT

Various morphologies of Co-containing precursors such as nanorods, nanosheets, and nanocubes were prepared by controlling the solvothermal reaction using cobalt acetate, L(+)-lysine, and oxalic acid, all of which were successfully converted into Co_3O_4 nanostructures without morphological variation. The gas responses of these Co_3O_4 nanosheets, nanorods, and nanocubes to 100 ppm C_2H_5OH at 300 °C were 10.5, 4.7, and 4.5 times higher than those of the Co_3O_4 agglomerated nanopowders, respectively. In addition, the selectivity to C_2H_5OH over CO and H_2, as well as the response/recovery kinetics, were significantly improved. These enhanced gas-sensing characteristics were attributed to the less agglomerated nanostructures of the sensing materials.

1. Introduction

Oxide semiconductor gas sensors show significant resistance change upon exposure to trace concentrations of toxic and explosive gases [1,2]. Since the discovery of oxide semiconductor gas sensors, the n-type semiconductors such as SnO_2 [3–5], ZnO [6,7], WO_3 [8,9], In_2O_3 [10,11], Fe_2O_3 [12], and TiO_2 [13–16] have been intensively studied as gas-sensing materials. In n-type semiconductors, the adsorption of negatively charged oxygen forms an electron depletion layer on the surface and the sensor resistance is increased. When the reducing gases are present in atmosphere, they are oxidized by the reaction with the negatively charged surface oxygen and the remnant electrons are injected into the semiconducting core, which decreases the sensor resistance significantly. In this resistive shell configuration, either the grain-boundary model or the neck model can be used to explain the change of sensor resistance [17].

In contrast, research on gas sensors using p-type oxide semiconductors is relatively limited. Thus far, gas sensors using CuO [18,19], Cr_2O_3 [20], and Co_3O_4 [21–28] have been reported. However, sensor performance and fundamental understanding are still in the elementary stage and further investigation is needed to improve the gas-sensing characteristics and elucidate the gas-sensing mechanism. Among p-type oxide semiconductors, Co_3O_4 is a promising material for applications to electrode materials in Li-ion batteries [21,29], catalysts [30,31], and gas sensors [21–28]. In particular, the oxidative catalytic activity of cobalt oxide is relatively well-known [30,31], and can be used to design or enhance the gas response, selectivity, and gas response kinetics. Indeed, several studies have investigated improved gas-sensing characteristics by the addition of cobalt oxide to the n-type semiconductors [32–38]. The main results include the increase of gas response [34–38], enhancement of response speed [36,37], and improvement of selectivity [34,37,38]. These show the potential of Co_3O_4 as a promising gas-sensing material having a different gas response, selectivity, and response kinetics.

The gas-sensing characteristics are also influenced greatly by the morphology, dimension, and nano-porosity of nanostructures [28,39–43]. Thus, it is worthwhile to study the gas-sensing characteristics of p-type Co_3O_4 with various morphologies and nanostructures. In this contribution, we prepare various Co_3O_4 nanostructures such as one-dimensional (1D) nanorods, 2D nanosheets, and 3D nanocubes by the solvothermal self-assembly reaction and measure the gas-sensing characteristics to C_2H_5OH, CO and H_2. The main study goals are to understand the enhanced gas-sensing characteristics by controlling morphology and elucidate the gas-sensing mechanism.

2. Experimental

Precursor powders were prepared under three different conditions to manipulate their morphologies. The sample specifications

* Corresponding author. Tel.: +82 2 3290 3282; fax: +82 2 928 3584.
E-mail address: jongheun@korea.ac.kr (J.-H. Lee).

0925-4005/$ – see front matter © 2010 Elsevier B.V. All rights reserved.
doi:10.1016/j.snb.2010.02.050

Table 1
The sample specifications and experimental conditions.

Specification	$[Co(C_2H_3O_2)_2]$	[L(+)-Lysine]	[Oxalic acid]	SRT[a]
CL-18	0.01 M	0.01 M	–	18 h
CO-1	0.01 M	–	0.01 M	1 h
CO-18	0.01 M	–	0.01 M	18 h
CLO-18	0.01 M	0.01 M	0.01 M	18 h

Specification	$[Co(C_2H_3O_2)_2]$	[Hyrazine]	[Oxalic acid]	Reaction time
CHO	0.01 M	1 ml	0.01 M	–

[a] Solvothermal reaction time.

are given in Table 1. The CLO-18 precursors (see Table 1) were prepared by the following process. The 25 ml of distilled water was mixed to 25 ml of ethanol (J.T. Baker Co., Ltd.), after which 0.088 g of $Co(C_2H_3O_2)_2$ (99.995% Sigma–Aldrich Co., Ltd., USA) was completely dissolved in the mixed solvents. Subsequently, 0.082 g of L(+)-lysine monohydrate (99%, Acros Organics) and 0.063 g of oxalic acid (99.5%, Kanto Chemical Co., Inc.) were added to the solution in sequence and stirred for 5 min. This stock solution was transferred to a Teflon-lined stainless steel autoclave (volume: 100 cm^3), which was then sealed and heated at 180 °C for 18 h. After cooling, the resulting product was washed five times with ethanol using a centrifuge and then dried at 70 °C for 1 day. The CL-18 precursors were prepared by the solvothermal reaction of the stock solution containing 0.088 of $Co(C_2H_3O_2)_2$ and 0.082 g of L(+)-lysine monohydrate. The CO-1 and CO-18 powders were prepared by the solvothermal reaction of the stock solution containing $Co(C_2H_3O_2)_2$ and oxalic acid for 1 and 18 h, respectively. Well-defined 1D, 2D and 3D Co_3O_4 nanostructures could be prepared by heat-treating above precursors. In order to investigate the influence of Co_3O_4 nanostructures with special morphology on the gas-sensing characteristics, the agglomerated configuration of Co_3O_4 powders were also prepared by heat-treating CHO precursors and its gas-sensing characteristics were measured. The CHO precursors were prepared at room temperature without solvothermal reaction. They were prepared by adding 0.088 g of $Co(C_2H_3O_2)_2$, 1 ml of hydrazine monohydrate (80.0% Samchun Pure Chemical Co., Ltd.) 1 cm^3, and 0.063 g of oxalic acid in sequence to the mixture of ethanol and distilled water.

The phase and crystallinity of the powders were analyzed by X-ray diffraction (XRD, Rigaku D/MAX-2500 V/PC), the morphologies of the precursors and powders by field-emission scanning electron microscopy (FE-SEM, S-4800, Hitachi Co. Ltd., Japan), and the surface areas of the powders by using the Brunauer–Emmett–Teller (BET) method (Tristar 3000, Micromeritics Co. Ltd.). The as-prepared precursors were prepared into a paste form and applied to an alumina substrate having two Au electrodes. The sensor element was heat treated at 400 °C for 1 h to convert the Co precursors into Co_3O_4 nanostructures and to decompose the organic content of the paste. The sensor was placed in a quartz tube and the temperature of furnace was stabilized at 300 °C. A flow-through technique with a constant flow rate of 500 cm^3/min was used. The Co_3O_4 sensor showed p-type semiconducting behavior in that the sensor resistance increased upon exposure to reducing gases. Thus, the gas response ($S = R_g/R_a$, R_g: resistance in gas, R_a: resistance in air) was measured at 300 °C. The dc 2-probe resistance of the sensor was measured using an electrometer interfaced with a computer.

3. Results and discussion

3.1. X-ray diffraction (XRD) analysis

The phases of the as-prepared precursors and Co_3O_4 nanostructures after heat treatment (HT) at 400 °C for 1 h in air were investigated using XRD. As prepared CL-18 precursors were crystalline $Co(OH)_2$ (JCPDS #74-1057) (not shown). The CO-1, CO-18, CLO-18 and CHO precursors showed crystalline diffraction patterns (not shown). However, the phases could not be identified from the JCPDS cards. The precursors were successfully converted into crystalline Co_3O_4 after HT at 400 °C for 1 h (Fig. 1(a)–(e)).

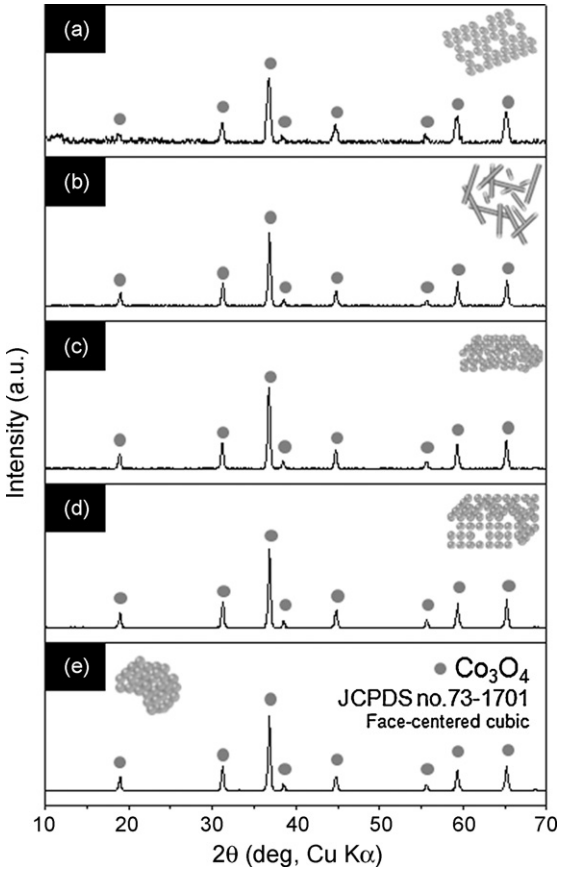

Fig. 1. X-ray diffraction (XRD) patterns of the Co_3O_4 nanostructures prepared by heat treatment (HT) of the precursors at 400 °C for 1 h: (a) Co_3O_4 nanosheets prepared by HT of CL-18 precursors, (b) Co_3O_4 nanorods prepared by HT of CO-1 precursors, (c) Co_3O_4 nanocubes prepared by HT of CO-18 precursors, (d) Co_3O_4 nanocubes prepared by HT of CLO-18 precursors, and (e) Co_3O_4 powders prepared by HT of CHO precursors.

3.2. Particle morphology

Fig. 2 shows scanning electron micrographs of the as-prepared cobalt precursors and the Co_3O_4 nanostructures after HT at 400 °C for 1 h. The morphologies of the cobalt precursors were closely dependent upon the additives of the stock solution. The as-prepared CL-18 precursors consisted of tiny nanosheets (Fig. 2(a)). Nanorods and nanocubes were observed in the CO-1 and CO-18 precursors, respectively (Fig. 2 (b) and (c)). The cubic morphology was also found in the CLO-18 precursors. In contrast, the CHO precursors prepared by room temperature reaction showed a ginkgo-nut-like morphology (Fig. 2(e)). All of these precursors were converted into Co_3O_4 nanostructures by HT without significant morphological change. These results indicated that the morphology of the Co_3O_4 nanostructures can be manipulated in the stage of solvothermal reaction.

The thickness of the Co_3O_4 nanosheets (~20 nm) (inset in Fig. 2(f)) was slightly thinner than the diameter of the Co_3O_4 nanorods (~ 30 nm) (inset in Fig. 2 (g)). The edge of the nanocubes was sized 1–2 μm (Fig. 2(h) and (i)). Most of the cobalt precursors

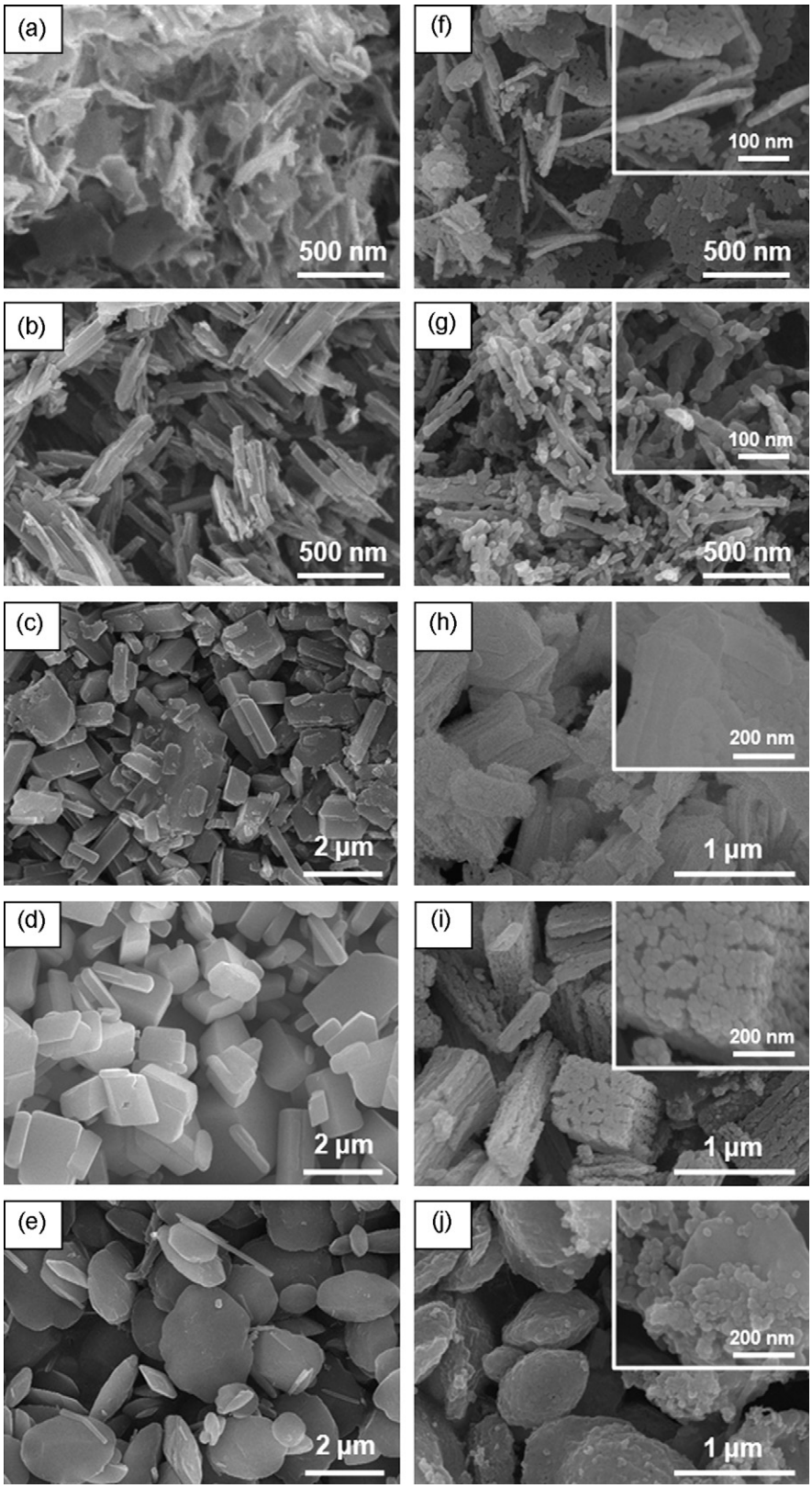

Fig. 2. SEM images of the as-prepared cobalt precursors and the Co_3O_4 nanostructures, the latter resulting from the heat treatment (HT) of the former at 400 °C for 1 h: (a) CL-18 precursors, (b) CO-1 precursors, (c) CO-18 precursors, (d) CLO-18 precursors, (e) CHO precursors, (f) Co_3O_4 nanosheets prepared by HT of CL-18 precursors, (g) Co_3O_4 nanorods prepared by HT of CO-1 precursors, (h) Co_3O_4 nanocubes prepared by HT of CO-18 precursors, (i) Co_3O_4 nanocubes prepared by HT of CLO-18 precursors, and (j) Co_3O_4 powders prepared by HT of CHO precursors.

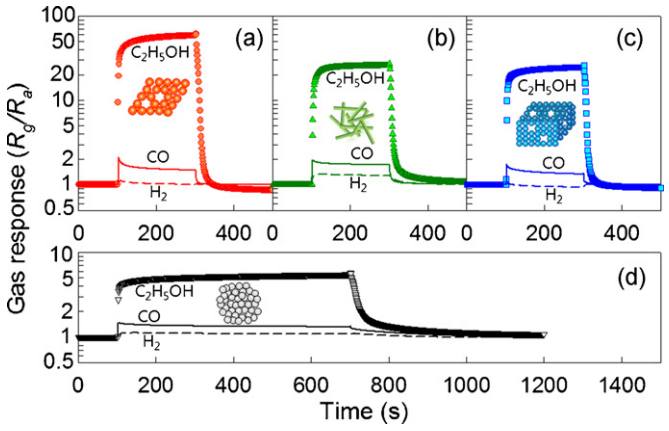

Fig. 3. Gas-sensing transients of (a) Co_3O_4 nanosheets, (b) Co_3O_4 nanorods, and (c) Co_3O_4 nanocubes to 100 ppm C_2H_5OH, 100 ppm H_2, 100 ppm CO and 1 ppm NO_2 at 300 °C. The nanosheets, nanorods, and nanocubes were prepared by HT of CL-18, CO-1 CLO-18 precursors at 400 °C for 1 h, respectively.

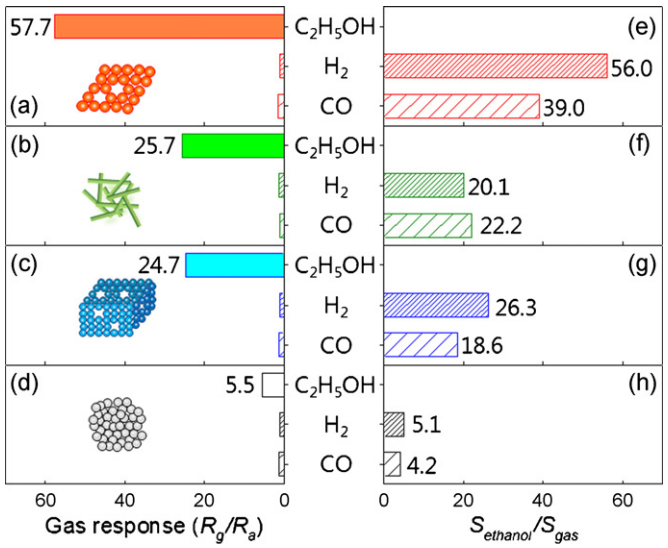

Fig. 4. Gas response (R_a/R_g) to 100 ppm C_2H_5OH, 100 ppm H_2 and 100 ppm CO at 400 °C and the selectivity to C_2H_5OH ($S_{ethanol}/S_{gas}$, $S_{ethanol}$ and S_{gas}: gas responses to C_2H_5OH and other gases, respectively): (a) and (e) Co_3O_4 nanosheets; (b) and (f) Co_3O_4 nanorods; (c) and (g) Co_3O_4 nanocubes; and (d) and (h) Co_3O_4 agglomerated powders.

were changed into nanoporous structures by HT at 400 °C (insets in Fig. 2(f)–(i)). The Co_3O_4 nanocubes prepared from the CLO-18 precursors (Fig. 2(i)) were more nanoporous than those prepared from the CO-18 precursors (Fig. 2(h)). Accordingly, the gas-sensing characteristics were measured for the Co_3O_4 nanosheets, nanorods, and nanocubes (Fig. 2(f), (g), (i)) prepared from the CL-18, CO-1, and CLO-18 precursors (Fig. 2 (a), (b), (d)), respectively. Note that the primary particles in the gingko-like Co_3O_4 powders were agglomerated in a relatively dense manner (Fig. 2(j)).

3.3. Gas-sensing characteristics and discussion

Fig. 3 shows the dynamic gas-sensing transients of the Co_3O_4 nanosheets, nanorods, nanocubes, and ginkgo-like agglomerated powders to 100 ppm C_2H_5OH, 100 ppm H_2, and 100 ppm CO at 300 °C. In all 4 sensors, the gas response to C_2H_5OH was high but was negligibly small to H_2 and CO. This is consistent with the literature data [23] although the reason for the selective detection of C_2H_5OH should be investigated more. The gas responses are summarized in Fig. 4. The gas responses to 100 ppm C_2H_5OH of the nanosheets, nanorods, and nanocubes were 57.7, 25.7, and 24.7 (Fig. 4 (a)–(c)), respectively, which were significantly higher than that of the gingko-like agglomerates (5.5) (Fig. 4(d)).

The gas response toward a specific gas needs to be markedly higher than those to other gases for selective gas detection. In order to quantify the selectivity to C_2H_5OH, the ratio between gas responses to C_2H_5OH and other gases ($S_{ethanol}/S_{gas}$) was calculated (Fig. 4 (e)–(h)). Higher $S_{ethanol}/S_{gas}$ values imply the more selective detection to C_2H_5OH in the presence of other gases. For example, $S_{ethanol}/S_{H2} = 56.0$ indicates that the gas response to C_2H_5OH is 56 times higher than that to H_2. The $S_{ethanol}/S_{H2}$ and $S_{ethanol}/S_{CO}$ values of the Co_3O_4 nanosheets, nanorods, and nanocubes ranged from 18.6 to 56.0, which were significantly higher than those of the Co_3O_4 agglomerates (4.2–5.1).

In particular, the Co_3O_4 nanosheets showed not only the highest gas response to C_2H_5OH but also the highest $S_{ethanol}/S_{H2}$ and $S_{ethanol}/S_{CO}$ ratios. To explain this result, the pore volume and surface area were measured (Fig. 5). The surface areas of the Co_3O_4 nanosheets, nanorods, nanocubes, and agglomerates were 43.6, 36.1, 26.2, and 19.3, respectively (Fig. 5(b)). The same order was also found in the pore volumes, with the nanosheets showing the highest pore volume (Fig. 5(a)). Thus, in general, the highest gas response of nanosheets was attributed to the greater chemical interaction with the sensing surface due to the higher surface area and pore volume. However, further investigation is needed to explain the highest selectivity of the nanosheets.

The high gas response of the Co_3O_4 nanostructures can be examined in more detail in relation to the possible gas-sensing

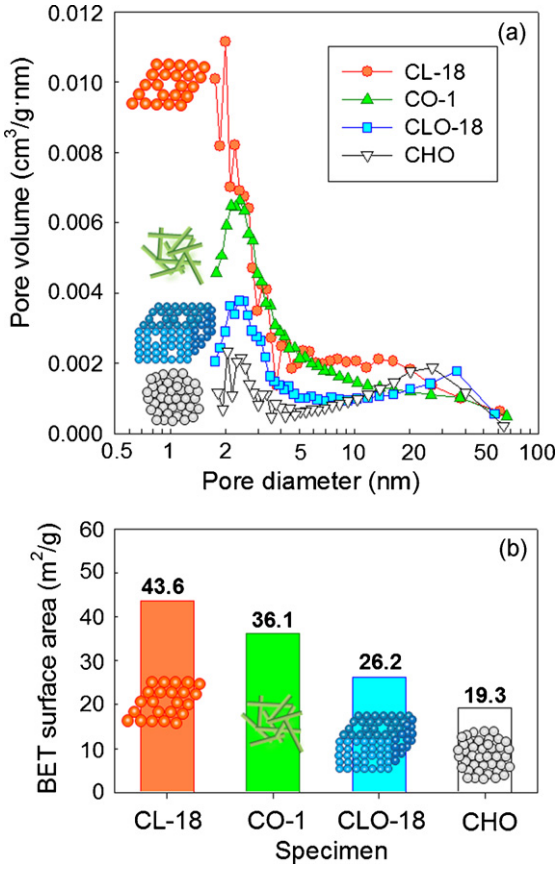

Fig. 5. (a) Pore size distributions and (b) BET surface area of the nanosheets, nanorods, nanocubes, and agglomerated powders prepared by the heat treatment (HT) of precursors at 400 °C for 1 h (determined from the nitrogen adsorption–desorption isotherm).

mechanism. The Co_3O_4 is a p-type semiconductor. The oxide surface of a p-type semiconductor is readily covered with chemisorbed oxygen, even at low oxygen partial pressure and even at temperatures up to 500 °C [44]. Thus, at the sensing temperature, the adsorption of negatively charged oxygen can generate the holes for conduction.

$$\frac{1}{2}O_2(g) \leftrightarrow O^-(ads) + h^\bullet \quad (1)$$

The following gas-sensing reactions might be considered according to the charges of the adsorbed oxygen species under the assumption of full oxidation of C_2H_5OH.

$$C_2H_5OH(g) + 6O^-(ads) + 6h^\bullet \rightarrow 2CO_2(g) + 3H_2O(g) \quad (2)$$

That is, the oxidation reaction with reducing gases increases the resistivity of the surface regions of the p-type Co_3O_4 nanostructures, which in turn increases the sensor resistance.

In the grain-boundary model of n-type semiconductors, the resistive contacts between the nanostructures dominate the sensor resistance, which is explained by the serial equivalent circuit model. Accordingly, the gas response is dependent upon the dimensions of the nanostructures, the surface area and the nano-porosity. By contrast, in the charge accumulation model of p-type semiconductors [45–47], the conduction occurs along the conductive surface. This can be explained in terms of the parallel equivalent circuit model. Although the gas-sensing mechanism of the p-type semiconductor is different, the total sensor resistance is also determined by the microstructural parameters such as surface area, nano-porosity, and the contact configuration between nanostructures. Hao et al. [20] reported that electrospun Cr_2O_3 nanofibers show substantially higher response to C_2H_5OH than do Cr_2O_3 powders. Park et al. [48] reported that Co_3O_4 hollow spheres with a shell thickness of ~40 nm show very high gas response to toluene and acetone vapor, whereas the gas responses of commercial Co_3O_4 powders are negligibly small. Liu et al. [49] reported that the gas responses of mesoporous Co_3O_4 films varied according to the change in interconnectivity. These findings support the close dependence of the gas responses on the nanostructures, not only in n-type but also in p-type semiconductors.

The times to reach 90% variation in resistance upon exposures to gas and air are defined as the 90% response time ($\tau_{90\%\text{-resp}}$) and the 90% recovery time ($\tau_{90\%\text{-recov}}$), respectively. The $\tau_{90\%\text{-resp}}$ values of the Co_3O_4 nanosheets, nanorods, and nanocubes were 66, 29, and 49 s, respectively, which are significantly shorter than that of the Co_3O_4 agglomerates (150 s) (Fig. 6(a)). The $\tau_{90\%\text{-recov}}$ values of the nanosheets, nanorods, and nanocubes ranged from 10 to 13 s, whereas that of the Co_3O_4 agglomerates was relatively long at 55 s (Fig. 6(b)).

Most gas sensors such as SnO_2, Fe_2O_3, TiO_2, In_2O_3, and WO_3 are n-type semiconductors and show a resistance decrease to reducing gases. In the literature, the response time of n-type semiconductor gas sensors upon exposure to reducing gases is shorter than the recovery time, regardless of the material [2,5,6,11,15]. This indicates that the gas-sensing reactions, including the in-diffusion of analyte gas and its subsequent oxidation with negatively charged adsorbed oxygen (O^- or O^{2-}), are generally shorter than a series of recovery reactions, including the counter-diffusion of oxidized product gases, the in-diffusion of oxygen gas to the surface, and the adsorption, dissociation, and ionization of oxygen. In particular, when less agglomerated and nanoporous sensing materials with enhanced gas diffusion are used [39], the surface reaction dominates the total recovery time.

The significantly long $\tau_{90\%\text{-resp}}$ and $\tau_{90\%\text{-recov}}$ values of the Co_3O_4 agglomerated powders in comparison to those of the Co_3O_4 nanosheets, nanorods, and nanocubes can be attributed to the restriction of gas diffusion. Further and more detailed study is required to explain why the $\tau_{90\%\text{-recov}}$ values are shorter than the $\tau_{90\%\text{-res}}$ values. However, we postulate the following as one possible explanation. The gas-sensing reaction (2) indicates that the adsorbed oxygens with negative charge and holes should be provided from the surface to oxidize the reducing gases. In the initial stage of the oxidation reaction, not only the negatively charged surface oxygen but also the holes just below the surface will be abundant and available for gas-sensing reaction. Taking into account the oxidative catalytic activity of Co_3O_4, in the later stage of gas sensing, the provision of sufficient holes or negatively charged surface oxygen can be considered as the limiting step that determines the response speed.

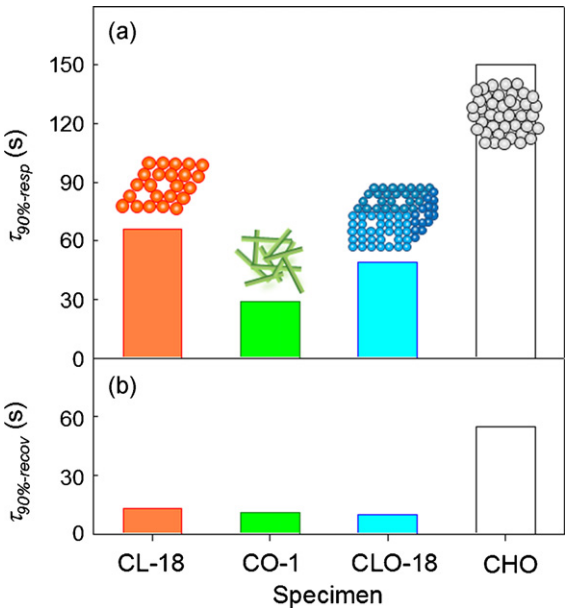

Fig. 6. (a) Ninety percent response time ($\tau_{90\%\text{-resp}}$) and (b) 90% recovery time ($\tau_{90\%\text{-rec}}$) of the nanosheets, nanorods, nanocubes, and agglomerated powders of the Co_3O_4 specimens at 400 °C.

The recovery reaction requires the counter-diffusion of oxidized gases and the subsequent hole generation by reactions (1). The gas diffusion in the less agglomerated Co_3O_4 nanostructures can be regarded as relatively fast, which is supported by the slow response/recovery speed in the agglomerated Co_3O_4 nanopowders. Accordingly, the hole generation reaction by (1) for the recovery reaction are thought to be more rapid than the oxidation reaction of reducing gases by (2).

4. Conclusions

Various Co_3O_4 nanostructures such as nanorods, nanosheets, and nanocubes were prepared by solvothermal self-assembly reaction and consequent heat treatment. The gas response and selectivity of the Co_3O_4 nanostructures with special morphology to 100 ppm C_2H_5OH were significantly higher than those of the Co_3O_4 agglomerated powders. In addition, the gas response and recovery times were significantly shortened by using well-defined Co_3O_4 nanostructures. The gas-sensing mechanism of the p-type Co_3O_4 nanostructures was discussed in relation to the microstructural factors such as surface area, nano-porosity, and contact configuration between the nanostructures. The enhanced gas-sensing characteristics were attributed to the effective and rapid diffusion of gases onto the entire surface of the less agglomerated and nanoporous Co_3O_4 nanostructures.

Acknowledgements

This work was supported by KOSEF NRL program grant funded by the Korean government (MEST) (No. R0A-2008-000-20032-0), a project, "Technologies development for future home appliance," and the Fundamental R&D program for Core Technology of Materials (M2008010013) funded by Ministry of Knowledge Economy.

References

[1] N. Yamazoe, Toward innovations of gas sensor technology, Sens. Actuators B 108 (2005) 2–14.
[2] Y. Shimizu, M. Egashira, Basic aspects and challenges of semiconductor gas sensors, MRS Bull. 24 (1999) 18–24.
[3] Y. Shimizu, A. Jono, T. Hyodo, M. Egashira, Preparation of large mesoporous SnO_2 powder for gas sensor application, Sens. Actuators B 108 (2005) 56–61.
[4] A. Kolmakov, Y. Zhang, G. Cheng, M. Moskovits, Detection of CO and O_2 using tin oxide nanowire sensor, Adv. Mater. 15 (2003) 997–1000.
[5] H.-R. Kim, K.-I. Choi, J.-H. Lee, S.A. Akbar, Highly sensitive and ultra-fast responding gas sensors using self-assembled hierarchical SnO_2 spheres, Sens. Actuators B 136 (2009) 138–143.
[6] Q. Wan, Q.H. Li, Y.J. Chen, T.H. Wang, X.L. He, J.P. Li, C.L. Lin, Fabrication and ethanol sensing characteristics of ZnO nanowire gas sensors, Appl. Phys. Lett. 84 (2004) 3654–3656.
[7] M.-W. Ahn, K.-S. Park, J.-H. Heo, J.-G. Park, D.-W. Kim, K.J. Choi, J.–H. Lee, S.-H. Hong, Gas sensing properties of defect-controlled ZnO-nanowire gas sensor, Appl. Phys. Lett. 93 (2008) 263103.
[8] T. Maekawa, J. Tamaki, N. Miura, N. Yamaoze, Gold-loaded tungsten-oxide sensor for detection of ammonia in air, Chem. Lett. 4 (1992) 639–642.
[9] C.–Y. Lee, S.–J. Kim, I.–S. Hwang, J.–H. Lee, Glucose-mediated hydrothermal synthesis and gas sensing characteristics of WO_3 hollow microspheres, Sens. Actuators B 142 (2009) 236–242.
[10] A. Gurlo, M. Ivanovskaya, N. Bârsan, M. Schweizer-Berberich, U. Weimar, W. Göpel, A. Diéguez, Grain size control in nanocrystalline In_2O_3 semiconductor gas sensors, Sens. Actuators B 44 (1997) 327–333.
[11] K.–I. Choi, H.–R. Kim, J.–H. Lee, Enhanced CO sensing characteristics of hierarchical and hollow In_2O_3 microspheres, Sens. Actuators B 138 (1997) 497–503.
[12] J. Chen, L.N. Xu, W.Y. Li, X.L. Gou, α-Fe_2O_3 nanotubes in gas sensor and lithium-ion battery, Adv. Mater. 17 (2005) 582–586.
[13] W.S. Choi, Y. Koo, Z. Zhongbin, Y. Li, D.-Y. Kim, Template synthesis of porous capsules with a controllable surface morphology and their application as gas sensors, Adv. Funct. Mater. 17 (2007) 1743–1749.
[14] O.K. Varghese, D. Gong, M. Paulose, K.G. Ong, E.C. Dickey, C.A. Grimes, Extreme changes in the electrical resistance of titania nanotubes with hydrogen exposure, Adv. Mater. 15 (2003) 624–627.
[15] I.D. Kim, A. Rothschild, B.H. Lee, D.Y. Kim, S.M. Jo, H.L. Tuller, Ultrasensitive chemiresistors based on electrospun TiO_2 nanofibers, Nano Lett. 6 (2006) 2009–2013.
[16] Y.-K. Jun, H.-S. Kim, J.-H. Lee, S.-H. Hong, CO sensing performance in micro-arc oxidized TiO_2 films for air quality control, Sens. Actuators B 120 (2006) 69–73.
[17] C. Xu, J. Tamaki, N. Miura, N. Yamazoe, Grain size effects on gas sensitivity of porous SnO_2-based elements, Sens. Actuators B 3 (1991) 147–155.
[18] J. Zhang, J. Liu, Q. Peng, X. Wang, Y. Li, Nearly monodisperse Cu_2O and CuO nanospheres: preparation and applications for sensitive gas sensors, Chem. Mater. 18 (2006) 867–871.
[19] Y.-S. Kim, I.-S. Hwang, S.-J. Kim, C.-Y. Lee, J.-H. Lee, CuO nanowire gas sensors for air quality control in automotive cabin, Sens. Actuators B 135 (2008) 298–303.
[20] R. Hao, J. Yuan, Q. Peng, Fabrication and sensing behavior of Cr_2O_3 nanofibers via in situ gelation and electrospinning, Chem. Lett. 35 (2006) 1248–1249.
[21] W.-Y. Li, L.-N. Xu, J. Chen, Co_3O_4 nanomaterials in lithium-ion batteries and gas sensors, Adv. Funct. Mater. 15 (2005) 851–857.
[22] C.–Y. Liu, C.–F. Chen, J.P. Leu, Fabrication of mesostructured cobalt oxide sensor and its application for CO detector, Electrochem. Solid-State Lett. 12 (2009) J40–J43.
[23] A.-M. Cao, J.-S. Hu, H.-P. Liang, W.-G. Song, L.-J. Wan, X.-L. He, X.-G. Gao, S.-H. Xia, Hierarchically structured cobalt oxide (Co_3O_4): the morphology control and its potential in sensors, J. Phys. Chem. B 110 (2006) 15858–15863.
[24] J. Wöllenstein, M. Burgmair, G. Plescher, T. Sulima, J. Hildenbrand, H. Böttner, I. Eisele, Cobalt oxide based gas sensors on silicon substrate for operation at low temperatures, Sens. Actuators B 93 (2003) 442–448.
[25] C. Cantalini, M. Post, D. Buso, M. Gulielmi, A. Martucci, Gas sensing properties of nanocrystalline NiO and Co_3O_4 in porous silica sol–gel films, Sens. Actuators B 108 (2005) 184–192.
[26] R.-J. Wu, C.-H. Hu, C.-T. Yeh, P.-G. Su, Nanogold on powdered cobalt oxide for carbon monoxide sensor, Sens. Actuators B 96 (2003) 596–601.
[27] S.-D. Choi, B.-K. Min, Co_3O_4-based isobutane sensor operating at low temperatures, Sens. Actuators B 77 (2001) 330–334.
[28] B. Geng, F. Zhan, C. Fang, N. Yu, A facile coordination compound precursor route to controlled synthesis of Co_3O_4 nanostructures and their room-temperature gas sensing properties, J. Mater. Chem. 18 (2008) 4977–4984.
[29] X.W. Lou, D. Deng, J.Y. Lee, J. Feng, L.A. Archer, Self-supported formation of needlelike Co_3O_4 nanotubes and their application as lithium-ion battery electrodes, Adv. Mater. 20 (2008) 258–262.
[30] X. Xie, Y. Li, Z.-Q. Liu, M. Haruta, W. Shen, Low-temperature oxidation of CO catalyzed by Co_3O_4 nanorods, Nature 458 (2009) 746–749.
[31] J. Jansson, A.E.C. Palmqvist, E. Fridell, M. Skoglundh, On the catalytic activity of Co_3O_4 in low-temperature CO oxidation, J. Catal. 211 (2002) 387–397.
[32] U.-S. Choi, G. Sakai, K. Shimanoe, N. Yamazoe, Sensing properties of Au-loaded SnO_2-Co_3O_4 composites to CO and H_2, Sens. Actuators B 107 (2005) 397–401.
[33] H. Yamaura, J. Tamaki, K. Moriya, N. Miura, N. Yamazoe, Highly selective CO sensor using indium oxide doubly promoted by cobalt oxide and gold, J. Electrochem. Soc. 144 (1997) L158–L160.
[34] H. Yamaura, K. Moriya, N. Miura, N. Yamazoe, Mechanism of sensitivity promotion in CO sensor using indium oxide and cobalt oxide, Sens. Actuators B 65 (2000) 39–41.
[35] U.-S. Choi, G. Sakai, K. Shimanoe, N. Yamazoe, Sensing properties of SnO_2–Co_3O_4 composites to CO and H_2, Sens. Actuators B 98 (2004) 166–173.
[36] S.B. Patil, P.P. Patil, M.A. More, Acetone vapour sensing characteristics of cobalt-doped SnO_2 thin films, Sens. Actuators B 125 (2007) 126–130.
[37] Z. Zing, S. Wu, Synthesis, characterization and gas sensing properties of undoped and Co-doped γ-Fe_2O_3-based gas sensors, Mater. Lett. 60 (2006) 952–956.
[38] H.-J. Lee, J.-H. Song, Y.-S. Yoon, T.-S. Kim, K.-J. Kim, W.-K. Choi, Enhancement of CO sensitivity of indium oxide-based semiconductor gas sensors through ultra-thin cobalt adsorption, Sens. Actuators B 79 (2001) 200–205.
[39] J.–H. Lee, Gas sensors using hierarchical and hollow oxide nanostructures: overview, Sens. Actuators B 140 (2009) 319–336.
[40] J. Liu, Z. Guo, F. Meng, Y. Jia, T. Luo, M. Li, J. Liu, Novel single-crystalline hierarchical structured ZnO nanorods fabricated via a wet-chemical route: combined high gas sensing performance with enhanced optical properties, Crystal Growth Des. 9 (2009) 1716–1722.
[41] E. Li, Z. Cheng, J. Xu, Q. Pan, W. Yu, Y. Chu, Indium oxide with novel morphology: synthesis and application in C_2H_5OH gas sensing, Crystal Growth Des. 9 (2009) 2146–2151.
[42] J. Xu, D. Wang, L. Qin, W. Yu, Q. Pan, SnO_2 nanorods and hollow spheres: controlled synthesis and gas sensing properties, Sens. Actuators B 137 (2009) 490–495.
[43] J. Xu, Y. Zhang, Y. Chen, Q. Xiang, Q. Pan, L. Shi, Uniform ZnO nanorods can be used to improve the response of ZnO gas sensor, Mater. Sci. Eng. B 150 (2008) 55–60.
[44] J. Hagen, Heterogeneous Catalysis: Fundamentals, Wiley-VCH, Weinheim, 1999, pp. 83–206.
[45] K. Sahner, R. Moos, M. Matam, J.J. Tunney, Hydrocarbon sensing with thick and thin film p-type conducting perovskite materials, Sens. Actuators B 108 (2005) 102–112.
[46] S. Pokrel, C.E. Simon, V. Quemener, N. Bârsan, U. Weimer, Investigation of conduction mechanism in Cr_2O_3 gas sensing thick films by ac impedance spectroscopy and work function changes measurements, Sens. Actuators B 133 (2008) 78–83.
[47] C. Wang, X.Q. Fu, X.Y. Xue, Y.G. Wang, T.H. Wang, Surface accumulation conduction controlled sensing characteristics of p-type CuO nanorods induced by oxygen adsorption, Nanotechnology 18 (2007) 145506.
[48] J. Park, X. Shen, G. Wang, Solvothermal synthesis and gas-sensing performance of Co_3O_4 hollow nanospheres, Sens. Actuators B 136 (2009) 494–498.
[49] C.–Y. Liu, C.–F. Chen, J.–P. Leu, Tunable interconnectivity of mesostructured cobalt oxide materials for sensing applications, Sens. Actuators B 137 (2009) 700–703.

Biographies

Kwon-Il Choi studied materials science and engineering and received his BS and MS degrees from Korea University in 2008 and 2010, respectively. He is currently a studying for a Ph.D. at Korea University. His research topic is the use of oxide nanostructures for chemical sensor applications.

Hae-Ryong Kim studied materials science and engineering and received his BS and MS degrees in 2005 and 2007, respectively, from Korea University. He is currently studying for a Ph.D. at Korea University. His research interest is oxide nanostructures for chemical sensor applications.

Kang-Min Kim studied materials science and engineering and received his BS degree from Kangwon National University, Korea, in 2004. In 2006, he received his MS degree from Korea University. He has worked for Samsung Corning and Samsung Corning Precision Glass Companies for 3 years. He is currently studying for a Ph.D. at Korea University. His research interest is oxide nanostructure-based solar cells.

Dawei Liu is studying for his Ph.D. in MSE department, University of Washington, his research interest is intercalation properties of lithium battery cathode.

Guozhong Cao is Boeing-Steiner Professor of Materials Science and Engineering at the University of Washington and received his Ph.D. degree from Eindhoven University of Technology (The Netherlands), MS from Shanghai Institute of Ceramics, and BS from East China University of Science and Technology (China). His recent research is focused mainly on synthesis and applications of nanomaterials for solar cells, lithium-ion batteries, catalysts, and sensors.

Jong-Heun Lee has been a Professor at Korea University since 2008. He received his BS, MS, and Ph.D. degrees from Seoul National University in 1987, 1989, and 1993, respectively. From 1993 to 1999, he developed automotive air-fuel-ratio sensors at the Samsung Advanced Institute of Technology. He was a STA (Science and Technology Agency of Japan) fellow at the National Institute for Research in Inorganic Materials (currently NIMS, Japan) from 1999 to 2000, a research professor at Seoul National University from 2000 to 2003, and an associate professor at Korea University from 2003 to 2008. His current research interests include chemical sensors, functional nanostructures, and solid oxide electrolytes.